Nano Research 11.12 (2018): 6405-6416

DOI: https://doi.org/10.1007/s12274-018-2165-y

Electrochemically Driven Phenothiazine Modified Carbon Nanodots

Mónica Mediavilla[a], Emiliano Martinez-Periñán[a], Iria Bravo[a,b], Tania García[a,b,c], Mónica Revenga-Parra[a,b,c], Félix Pariente[a,b,c] and Encarnación Lorenzo[a,b,c (*).]

[a] Departamento de Química Analítica y Análisis Instrumental, Universidad Autónoma de Madrid, 28049 Madrid, Spain.

[b] Instituto Madrileño de Estudios Avanzados (IMDEA) Nanociencia, Faraday, 9, Campus UAM, Cantoblanco, 28049 Madrid, Spain

[c] Institute for Advanced Research in Chemical Sciences (IAdChem), Universidad Autónoma de Madrid, 28049 Madrid, Spain.

ABSTRACT

Carbon nanodots (CNDs) with enriched periphery carboxylic groups were synthesized using a low-cost starting material such as glucose. The obtained CNDs were assembled on an Au electrode following two strategies: covalent bonding, using cystamine as a cross-linker, and by drop-casting. The immobilized CNDs were covalently modified with a phenothiazine, Azure A, via electron transfer chemistry, in particular via reactions with aryl diazonium salts. The reaction mechanism of diazonium functionalization of CNDs was investigated. Spectroelectrochemistry experiments assisted in corroborating that the electrografting, rather than adsorption, governs the Azure A carbon nanodots functionalization. Finally, an application for CNDs modified by this chemistry as electrocatalysts towards the oxidation of hydrazine is demonstrated.

KEYWORDS

Carbon nanodots, Azure A, electrografting, phenothiazine.

1 Introduction

Carbon nanodots (CNDs) are recently receiving significant attention due to the remarkable properties they present, such as low cost, excellent chemical stability[1], biocompatibility[2] and good photostability[2-4]. All these attributes make CNDs suitable for many analytical and bioanalytical applications such as fluorescent imaging or (bio)sensing[4-7].

Since CNDs initial discovery by arc-discharge methods[8], they have been studied and fabricated by several research groups trying to achieve better synthetic routes, deeper understanding of their physicochemical properties and to develop novel applications. The routes explored to prepare CNDs from affordable starting materials and without needing complicate experimental set-ups, are classified as top-down or bottom-up[9, 10].

Unlike other carbon nanomaterials, CNDs are rich in surface functional groups, which provide them not only with a high intrinsic solubility, but also with sites for further functionalization. Therefore, CNDs are ideal candidates for decoration with tailored functional groups through covalent bonds, endowing them with new functionalities. There are different motivations for chemical modification of CNDs, including changing its doping level, charge storage, chemical and biological sensing, making new composite materials, among others. However, although the covalent approach to CNDs functionalization is of special interest as it allows the insertion of multiple photo- or electroactive units forming stable nanoconjugates, it has been recently explored only with porphyrins[11, 12] and with □-extended tetrathiafulvalene (exTTF)[13]. Few reports can be found involving other interesting chemical reactions, such as the formation of C-C bonds by electroreduction of aryl diazonium salts. This reaction presents the advantage of not needing multiple intricate synthesis and purification of diazonium salts steps, which can bear a wide variety of functional groups, and also, of forming highly stable grafted layers[14-24]. The diazotization of functional groups also permits their immobilization onto conductive substrates, producing surfaces with modified or enhanced properties, which provide new or improved functions.

Electrochemical studies of CNDs have been previously reported[25, 26] but few works are related to their applications in electrochemical sensing[27-29], even less concerning the electrochemical modification, although the abundant active sites at the edge of CNDs and large surface area of the base plane are in favor of the electron transfer of CNDs, making them advantageous for electrochemical sensing. In this context, we have explored an electrochemical method for Azure A modification of CNDs immobilized on a gold electrode based on the electrografting of the Azure A diazonium salt. Modification of CNDs with interesting compounds, such as dyes, to tune their intrinsic properties and exploit new functions is attractive for many applications. Besides, we have carried out a detailed spectroelectrochemical study of the electrografting process in order to address questions about the mechanism and to stablish the optimal conditions to be performed. For this purpose, new capabilities afforded by in situ and operando methods may be very useful. Operando spectroscopy involves carrying out real-time measurements with spectrophotometric techniques. Among these UV-Vis absorption spectroelectrochemistry is a multi-response technique that allows to obtain simultaneously the electrochemical and the spectroscopic evolution of an electron-transfer process, in a single experiment[30-32]. It has become a useful technique for studying the mechanisms of electrochemical reactions due to its capability to investigate the reactivity of surface species under reaction conditions.

Finally, the activity of the electrografted phenothiazine was assessed by its application to the electrocatalysis of hydrazine.

2 Experimental

2.1 Reagents and apparatus.

Azure A chloride (AA), D(+)-Glucose, N-Hydroxysuccinimide (NHS), 1-ethyl-3-(3-Dimethylaminopropyl)carbodiimide (EDC), cystamine dihydrochloride and hydrazine were obtained from Sigma Chemical Co. Sodium nitrite was purchased from Riedel-de-Haën.

Carbon nanodots (CNDs) were synthetized by thermal carbonization of carbohydrates following the procedure previously described by Peng et al.[33]. Briefly, 2.0 g of D(+)-Glucose were dissolved in 5 mL of water. After that, 8 mL of H_2SO_4 were added and the mixture was stirred for 40 min. Then, 40 mL of water were added. After centrifugation (5000 rpm for 10 min.), the black carbonaceous powder produced was separated and washed with Milli-Q water and the supernatant solution removed. The process was repeated 4 times. The resulting carbon powder was dispersed in 50 mL of HNO_3 solution (2.0 M) and ultrasonicated for 30 min. This suspension was heated under reflux for 12 hrs. Once cooled to room temperature, the solution was neutralized with 20% Na_2CO_3 solution. The CNDs obtained were dialyzed for three days using a 3.5 kD dialysis membrane (Sigma PUR-A-LYZERTM MEGA 3500). The final suspension was kept refrigerated until use.

Electrochemical measurements were carried out using an Autolab PGSTAT 30 potentiostat (Eco-Chemie, The Netherlands) and were performed using integrated screen-printed gold electrodes (4 mm diameter, AuSPEs) (DropSens-Metrohm) that include a gold working, a silver pseudo reference and a gold counter electrode. The electrodes were connected using a SPE Connector (DropSens-Metrohm) as interface. The solutions were treated with prepurified nitrogen in order to remove the oxygen for the electrochemical measurements.

Spectroelectrochemical studies were carried out using the Spelec equipment (DropSens-Metrohm). In this system (Supporting Information, Fig. S1), the screen-printed electrode is placed in a Teflon cell, with a 100 µL capacity, in which an optical probe is inserted. All the experiments were carried out in a reflection mode. The probe consists of a series of optical fibers connected to the lamp, through which the incident beam is sent, or to the spectrometer where the output signal is processed. This system is equipped with a Bipotentiostat/Galvanostat (± 4 V DC potential range, ± 40 mA maximum measurable current) and a Spectrometer wavelength range: 200-900 nm. Both electrochemical and optical systems are controlled using the DROPVIEW SPELEC Software, allowing to register simultaneously spectroscopic and electrochemical signals in a single experiment.

Dynamic Light Scattering (DLS) measurements were carried out in a VASCO Particle Size Analyzer (Cordouan Technologies) at 25 °C. Transmission electron microscopy (TEM) images were obtained with a FEG S/TEM (Talos F200X, FEI) electron microscope. Elemental analysis was conducted in a Perkin-Elmer 2400 CHN Elemental Analyzer. Atomic force microscopy (AFM) studies were carried out in an Agilent 5500 microscope operating in tapping mode in air. Olympus cantilevers (RC800PSA, 200_20 mm) with a tip radius of ca. 20 nm and spring constants of 0.15-0.6 Nm-1 were employed. WSxM software (www.wsxmsolutions.com) was employed both for data acquisition and image processing [34]. For these studies gold covered (200–300 nm thick) glass plates (Arrandee Co. Werther, Germany) were used. Before use, gold surfaces were annealed in a gas flame to generate Au (111) terraces. Fourier transform

infrared spectroscopy (FTIR) spectrum was recorded on KBr pressed pellets from 5000 to 500 cm-1 using a Brucker IFS60v spectrometer. UV–vis absorption spectrum was recorded in a double beam PharmaSpec UV-1700 series from Shimadzu Corporation, operating from 200 to 800 nm in 1.0 cm quartz cells. Fluorescence emission spectroscopy was carried out on a Cary Eclipse Varian spectrofluorimeter.

2.2 Procedures.

2.2.1 In situ generated diazotized Azure A.

Diazotization of Azure A was performed in an ice bath by mixing equal volumes of 2.0 mM Azure A (in 0.2 M HCl) and 2.0 mM $NaNO_2$ in water. After keeping this solution at 4 °C for a minimum of 10 minutes it was used for electrode modification.

2.2.2 Electrode activation.

AuSPEs were electrochemically activated by potential cycling (5 times) from -0.10 to 1.20 V at 0.10 Vs-1 in a 0.1 M H_2SO_4 solution. Then, the electrodes were washed with purified water. After that, the electrode was ready for modification.

2.2.3 Electrode modification with CNDs.

Activated AuSPEs were modified with CNDs (CNDs/AuSPE) by the following procedures: 1) Adsorption: by drop-casting aliquots of 14 µL onto the working electrode. After 120 minutes, the solvent was evaporated (at room temperature) and the modified electrodes were ready for use. 2) Covalent attachment: 15 µL of 100 mM cystamine in aqueous solution were drop-casted on the gold electrode. Electrodes were kept at dark during 20 hrs. Afterwards, they were rinsed with water and 10 µL of a mixture of 1 mM NHS, 1 mM EDC and 50 µL of CNDs were deposited onto the electrodes, which were kept in a moist chamber at 4 °C for 3 hours. Then, they were rinsed with distilled water and stored at room temperature in the dark until their use.

2.2.4 CNDs modification with Azure A diazonium salt.

Grafting of the dye diazonium salt on the CNDs was performed in the diazotization solution by cycling the potential of CNDs/AuSPE from +0.50 V to -0.25 V at 0.10 Vs-1 to electrochemically reduce the in situ generated Azure A diazonium salt. After rinsing the resulting modified electrodes (AA/CNDs/AuSPE) with water, they were electrochemically conditioned by applying a serial of potential scans between -0.40 V and +0.60 V at 0.10 Vs-1 for 10 min. in the corresponding electrolyte (0.1 M HCl or 0.1 M phosphate buffer solution pH 7.0 (PB)). This conditioning step was carried out in order to eliminate the weakly adsorbed material onto the electrode surface.

3. Results and Discussion.

CNDs were prepared by thermal carbonization of D(+)-Glucose as described in the experimental section. Independent physicochemical characterization was performed using UV-Visible absorption spectrophotometry, Fluorescence spectrophotometry, Fourier transform infrared spectroscopy (FT-IR), Dynamic light scattering (DLS), Elemental analysis and Transmission electron microscopy (TEM). The as-prepared nanodots have an average size of 2.2 nm, as indicated by the size distribution obtained by DLS measurements (Fig. 1A), in which, sizes varied from 1.9 to 3.2 nm. This value is corroborated by TEM images, in which it can be observed that CNDs sizes range from 2 to 5 nm (Fig. 1B,C). Through Fast Fourier Transform

(FFT) analysis of the images a spacing of the planes of 2.5 Å was obtained, corresponding to the (100) plane of CNDs (Fig. 1D).

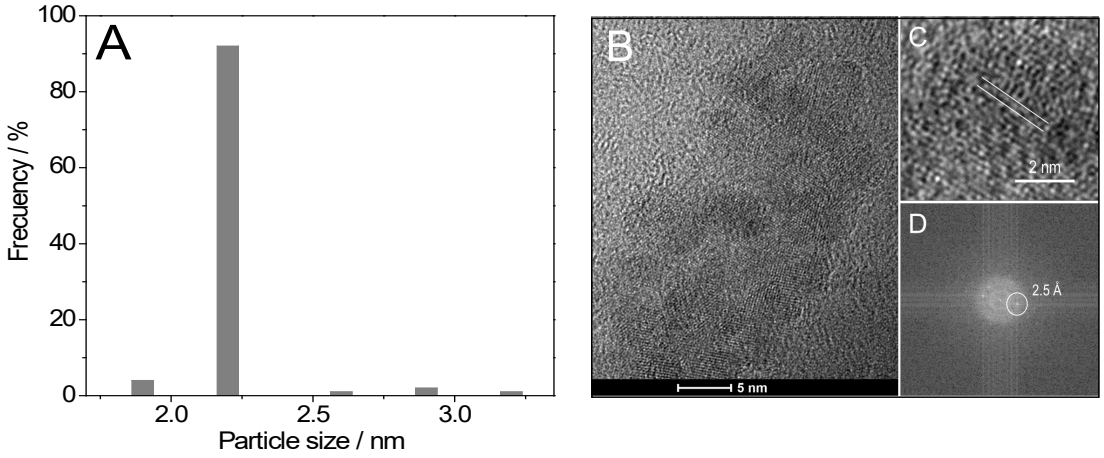

Figure 1. (A) Dynamic light scattering histogram of CNDs. (B) TEM images of the synthetized CNDs (B, C). FFT analysis of the images (D).

The composition of CNDs was confirmed by elemental analysis. The results obtained were: 17.51% C, 7.84% N and 2.32% H. The FTIR spectrum was used to investigate the surface functional groups of CNDs (Fig. S2). The broad bands between 3000 and 3500 cm-1, corresponding to O-H and N-H stretching, along with the band at 1650 cm-1, ascribed to C=O stretching, confirm the presence of -COOH groups, what could explain the good water-solubility of CNDs. Bands around 2900 cm-1 are assigned to C-H stretching vibrations and the ones around 1050 cm-1 correspond to C-O-C/C-O bonds. Finally, the band at 1400 cm-1 could be due to C=C or C-N stretching vibrations. These results confirm the presence of carboxyl groups on the surface of the CNDs.

The optical properties of CNDs were also studied by UV-Vis absorption and fluorescence spectroscopy. The UV-Vis absorption spectrum shows a broad peak around 300 nm (Fig. 2A). In the fluorescence spectrum displayed in Fig. 2B a narrow and symmetric emission band at 446 nm can be seen when the excitation wavelength is set at 340 nm. The emission maximum shifts to the blue on increasing the excitation wavelength (Fig. 2B). The width at a half maximum at the different excitation wavelengths remains almost constant, what confirmed a narrow size distribution of the as-prepared CNDs. Therefore, the fluorescence dependence on excitation wavelength observed can be due to the different emissive sites of the different functional groups that are surrounding the CNDs rather than to CNDs different sizes[35].

The relative fluorescence quantum yield of CDNs was determined in water by measuring fluorescence of quinine at the same experimental parameters as CNDs. Applying the following equation 1:

(1)

$$\varphi_x=\varphi_{st}\,(m_x/m_{st})((\eta_x^2)/(\eta_{st}^2))$$

the quantum yield was found to be 1%.

CNDs were stable over several days as it is deduced from the fluorescence spectra, that remains unchanged within the experimental error (data not shown). This indicates that no photochemical reactions in the stock solutions seem to occur, which is very useful for further applications.

Based on the results obtained from the different characterization techniques employed, it can be concluded that the CNDs were successfully synthesized.

AuSPE electrode were modified with CNDs (CNDs/AuSPE) by the adsorption and covalent attachment procedures described in the experimental section. Following the covalent attachment procedure, the gold electrode surface was covalently modified with CNDs. For that purpose, a cystamine self-assembled monolayer (SAM) was formed on the gold electrode, thus providing amine terminal groups, which can be used to attach the carboxylic groups of CNDs by forming amide bonds.

The electrochemical behavior of CNDs/AuSPE electrodes was studied by cyclic voltammetry. The distinctive cyclic voltammetry response of AuSPE in 0.1 M H2SO4 is altered when the electrode is modified with CNDs (Fig. S3). The oxidation peak current is increased and the potential is shifted to more positive values. Moreover, the sharp reduction peak decreases and the potential is shifted to higher values. These effects are consistent with an alteration of the gold surface after modification with CNDs. In 0.1 M PB pH 7.0 solution no redox peaks are observed in the potential window studied.

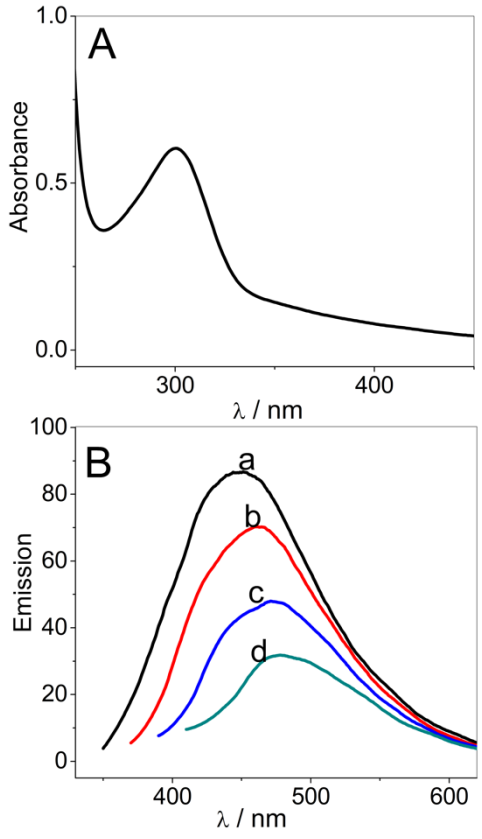

Figure 2. (A) Absorption and (B) Fluorescence emission spectra of the CNDs in water at different excitation wavelengths: (a) 340, (b) 360, (c) 380 and (d) 400 nm.

The electrografting of aryl diazonium molecules onto conducting substrates can be carried out using a potential assisted reaction. The diazonium functional group electroreduction produces extremely reactive aryl radicals that covalently bind to the conducting surface, releasing a nitrogen molecule[36]. Hence, the electrografting of Azure A diazonium salt onto CNDs, immobilized on the gold electrode surfaces by both strategies, was carried out in 0.1 M HCl by potential cycling (+0.50 V to -0.25 V) at 0.10 Vs-1 during 5 cycles. Fig. 3 shows the cycle number 5. It can be observed that no matter the CNDs immobilization strategy used, once the first cathodic scan is completed, two electrochemical processes appear. The first one well-defined redox process centered at +0.10 V can be attributed to the aryl diazonium moiety and the cationic dye simultaneous reduction. The second redox process, at around 0.00 V, is less defined and it is related to the unspecifically adsorbed Azure A molecules. Since the same process around 0.00 V is observed for a solution of Azure A in 0.1M HCl (Fig. S4), the oxidation process is rather due to the oxidation of the cathionic dye than to the unreacted diazo derivative of the Azure A, since the last is unstable. As consecutive potential scans are applied, a decrease in the peak current can be observed, however the peak potential remains constant. These results suggest that an Azure A film is growing on the CNDs and it becomes less conductive as it grows. Hence, it will result on the formation of an CNDs/AuSPE modified with Azure A, either if CNDs are adsorbed or covalently attached to the Au surface.

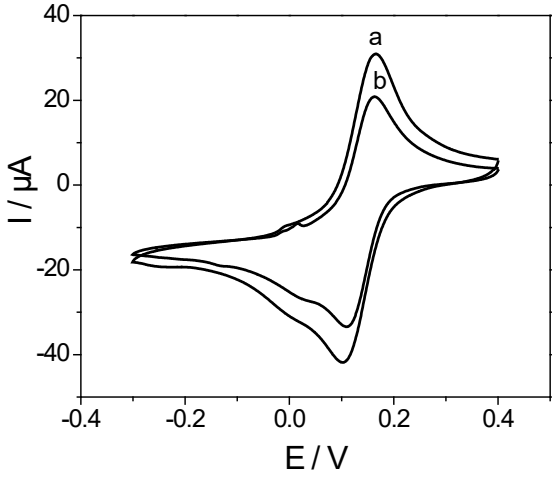

Figure 3. Cyclic voltammograms of the electrografting of 1.0 mM Azure A diazonium salt at a CNDs/AuSPE prepared following the adsorption (a) or covalent attachment (b) procedure as indicated in the experimental section in 0.1 M HCl at 0.10 V s-1. The figure shows the fifth voltammogram of potential cycling.

After five potential scans in the electrografting step, the electrode was removed from the cell, washed with water and immersed in 0.1M HCl or 0.1M PB pH 7.0 electrolyte, in the absence of Azure A, a voltammetric response, typical of a quasi-reversible redox couple confined on the electrode surface, is observed at 0.13V or -0.38 V, respectively (Fig. 4A and B). This surface-confined electrochemical process is ascribed to the immobilized cationic dye oxidation/reduction. As one would expect, the formal potential E0 shifts to more negative

value on increasing pH, since the redox response of Azure A is pH dependent [37-39]. Moreover, the voltammetric response is much higher in 0.1 M HCl, which indicates that protons are involved in the electrochemical reaction.

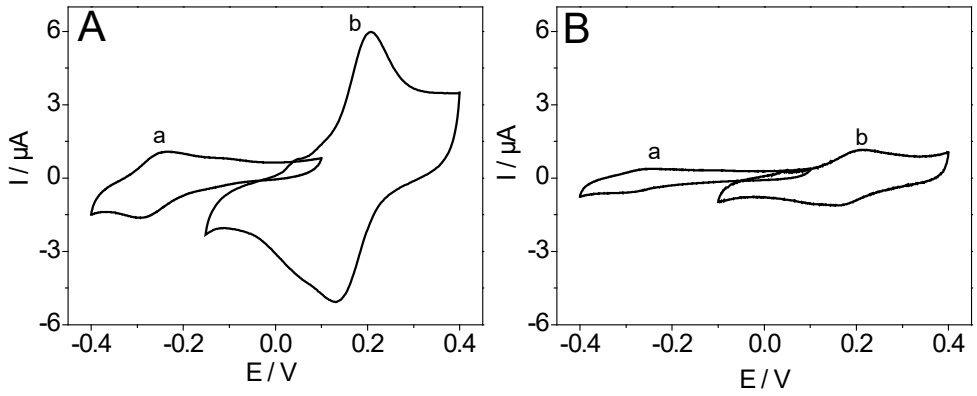

Figure 4. Cyclic voltammograms of a CNDs/AuSPE prepared following the adsorption (A) or covalent attachment (B) procedure modified with films derived from electrografted Azure A recorded in 0.1M PB pH 7.0 (a) or 0.1M HCl (b) at 0.10 Vs-1.

The results described above indicate that CNDs have been modified with Azure A by a grafting process electrochemically driven either when the nanomaterial has been just adsorbed or covalently bonded to the electrode surface. To confirm that the electrografting takes place on CNDs but not on the gold surface, similar experiments to those described above were carried out on plain AuSPEs. Although the cyclic voltammetric response of Azure A diazonium salt in 0.1 M HCl is similar to that observed for CNDs/AuSPEs, when after 5 consecutive cycles the electrode is removed from the solution, rinsed with water and placed in a solution containing only electrolyte without Azure A diazonium salt, no voltammetric response is observed (data not shown). Based on these results it can be concluded that Azure A molecules are grafted onto the CNDs present at the CNDs/AuSPE surface via the formation of a C – C bond. Moreover, from Fig. 4 it can also be concluded that a higher amount of Azure A is electrografted when CNDs are just adsorbed on the electrode surface compared to the covalently bonded CNDs. From the area under the voltammetric wave obtained at 0.1 M HCl for three electrodes modified with electrografted Azure A, we have estimated a surface coverage of (1.3±0.1) x 10-11 and (5.3±0.5) x 10-12 mol/cm2 for CNDs just adsorbed or covalently bonded on AuSPEs, respectively. Hence, based on these results it seems that adsorption gives rise to higher CNDs surfaces coverages, onto which higher amount of Azure A will be further grafted.

The same experiment was then performed in a non-diazotized Azure A solution. In this case, the anodic and cathodic electrochemical processes can be seen, maintaining its diffusion-like behavior (Fig. S4A). In the cathodic scan an adsorption contribution also appears. Moreover, in the subsequent scans in phosphate buffer no voltammetric response was observed (Fig. S4B), demonstrating the importance of the previous diazotization step in the electrografting process as well as that the resultant film is principally composed of electrochemically grafted molecules.

As we mentioned above, the electrografted Azure A films show the behavior expected for a surface-confined redox process. Up to 0.40 Vs-1, the peak currents kept a linear relationship with the scan rate. Nevertheless, for scan rates higher than 0.50 Vs-1, ΔEp values underwent a significant increase, what suggests that there exists a charge transfer kinetics limitation. From the peak potential variation with the scan rate, the charge transfer features of the Azure A electrografted films obtained on adsorbed or covalent bonded CNDs were determined at pH 7.0 according to the Laviron formalism[40]. The electron transfer coefficient (α) and the electron transfer rate constant (ks) were found to be 0.57 and 153 s-1 for adsorbed CNDs and 0.53 and 43 s-1 for covalent bonded CNDs, respectively. These results indicate that Azure A films obtained on electrodes modified with CNDs by adsorption show faster charge-transfer kinetics than those modified by covalent binding. This can be explained by considering that the adsorbed CNDs facilitate the electron transfer between the Azure A electrografted film and the electrode surface compared to the covalent bonded CNDs through a previously formed self-assembled monolayer of cystamine. Considering this result, for following studies we have chosen the CNDs drop-casting method for electrode modification.

The generation of the grafted Azure A film is expected to be affected by different experimental conditions, such as the concentration of Azure A or the number of potential scans, and thus, they were optimized. 0.5, 1.0 and 5.0 mM Azure A was assayed cycling the potential from 5 to 50 times. There is a self-limitation in the film growth owing to a gradual covering of the electrode surface, thus hindering the access to new diazotized molecules. Best results, in terms of electron transfer properties and stability of the resulting films with stable coverage upon potential cycling, were obtained at 1.0 mM Azure A and 5 potential cycles. Few cycles (2-3) give rise to Azure A modified electrodes with low surface coverages. Increasing the number of cycles the film grows, by forming multilayers, but it becomes more insulating.

In order to characterize the nature of the resulting CNDs modified AuSPEs obtained either by direct adsorption or covalent bonding and to stablish the differences between them, we have carried out AFM experiments, which provide morphological information that complete the results obtained by CV. Fig. 5 shows an image of CNDs-modified gold substrate prepared following the adsorption (A) or covalent attachment (B) procedure. Images exhibit a morphology with granular structures ascribed to the CNDs. In the case of direct adsorption, they are homogeneously distributed over the surface giving rise to quite compact layers. The tendency of the CNDs to aggregate lead to large structures of about 7 nm in size. When the CNDs have been covalently bonded (Fig. 5B), the granular structures are not as neat as in the adsorption case. In fact, the image is somehow blurred with respect to that obtained on the adsorbed CNDs surface. Structures in the 2-3 nm range are detected. In this case the CNDs are anchored onto the cystamine layer, the size agrees well with the size estimated by TEM. This fact suggests that the CNDs immobilization geometry is not the same for both systems. In the case of the covalently bonded CNDs, the distribution seems to have a certain order compared to the distribution observed on adsorbed CNDs surface, but with a lower CNDs surface coverage.

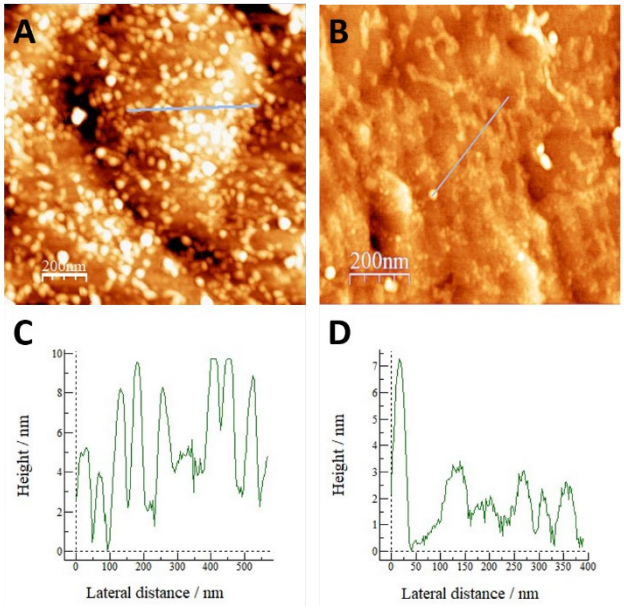

Figure 5. AFM images of CNDs modified gold surfaces prepared by adsorption (A) or covalent attachment (B). Height profiles of adsorption (C) and covalent attachment (D) procedure.

In order to obtain a complete and detailed overview of the electrografting process, operando measurements, which refers to the simultaneous characterization of both the physico-chemical properties and activities of the process under actual reaction conditions, are also required. In UV-Vis spectroelectrochemistry experiments of the Azure A electrografting process by reflection mode, signals of different nature are obtained at the same time, giving an overview about the changes that take place in solution, at the electrode surface, or in both of them, during the course of a reaction. For these studies, the dye concentration employed was lower than that used in the above described electrochemical studies in order not to saturate the UV-Vis detector. 62.5 µM Azure A or 62.5 µM Azure A diazonium salt in 0.1 M HCl were used at the electrode platforms studied CNDs/AuSPE and bare AuSPE (used as comparison). Fig. 6 shows the first cyclic voltammogram scan obtained with a bare AuSPE (Fig. 6A) and a CNDs/AuSPE (Fig. 6B) in a solution containing 62.5 µM Azure A. In both cases, a redox couple at E0 = +0.07 V appears. The cathodic peak presents two contributions ascribed to the diffusional and adsorption process of Azure A at +0.08 V and +0.04 V, respectively. The adsorption contribution is higher than the diffusional one when CNDs are present on the AuSPE surface. Higher cathodic and anodic peaks are observed in the presence of CNDs which could be attributed to the fact that the nanomaterial increases the electroactive area and promotes the electron transfer in the electrochemical process. The corresponding UV-Vis spectra showing the absorbance variation are presented in Fig. 6E and F. In both cases, when the reduction process occurs the absorbance of the wide band, with two defined peaks at 590 nm and 630 nm, decreases. This phenomenon is associated with the absorbance decrease of the main band observed in the Azure A spectrum (Fig. S5), ascribed to the Azure Aox species. As the Azure Aox is reduced during the electrochemical process, its absorbance band decreases since the Azure Ared formed does not absorb at the same wavelength. As the cathodic potential scan moves forward, the absorbance of the main bands (590 nm and 630 nm) decreases, even at the beginning of the anodic scan where the potentials are lower than the potential at which the oxidation process takes place. Once the oxidation process begins,

the absorbance increases in a positive sign, but the initial absorbance value is not completely recovered, pointing out that the process is not completely reversible. The CNDs/AuSPEs show a similar voltammetric behavior, but changes in absorbance are greater. This fact is associated with the better electron transfer during Azure Aox reduction as it is shown at the CV. In order to study the electrografting process, the same study was carried out using a solution of 62.5 µM Azure A diazonium salt. The cyclic voltammograms during the cathodic scans show a first peak around +0.14 V (Fig. 6C and D), associated with the electrografting process of the aryl diazonium salt, and a second peak at +0.05 V ascribed to the reduction of the phenothiazine Azure Aox to Azure Ared. The presence of CNDs produces an increase of the cathodic and anodic peaks, as consequence of the higher electroactive area caused by the carbon nanomaterial on the electrode surface. Regarding to the spectroscopy results (Fig. 6G and H), in both cases, a band at 630 nm, that increases while the two cathodic processes occur, is observed. This band is ascribed to the electrografted Azure A on the AuSPE or on the CNDs/AuSPE after the reduction of aryl diazonium salt. However, the band at 430 nm, ascribed to the diazo group, decreases during the cathodic process, which is consistent with the consumption of Azure A diazonium salt and the generation of Azure A electrografted on the electrode surface. The absorption band at 550 nm, also associated with the reduction of the aryl diazonium salt process, firstly decreases during the cathodic scan and then slightly recovers during the anodic one.

A more in-depth study of the spectroelectrochemical data was carried out focusing on the absorbance variation (ΔAbs) of the main bands (430, 550 and 630 nm) vs. the applied potential (voltabsorptogram) (Fig. S6 A, B and C). At 430 nm (Fig. S6A), for both electrodes under study (bare AuSPE and CNDs/AuSPE) ΔAbs decreases by the same magnitude, almost no effect of CNDs was observed. The absorbance at this wavelength decreases on successive potential scans. This fact is consistent with the decrease of the Azure A diazonium salt concentration as it is electrografted onto the electrode surface during the potential cycling. The analysis of the derivative of the voltabsorptogram of the first scan (Fig. S6D) shows an irreversible peak around at +0.10 V, close to the potential at which the cathodic peak appears in the cyclic voltammogram (Fig. 6C and D). This indicates that the absorbance variation at 430 nm is due to the electroreduction of the aryl diazonium salt. No peaks are observed in the voltabsorptograms during the anodic scan, confirming the irreversibility of the process once the Azure A diazonium salt molecule is electrografted on the electrode surface. ΔAbs at 550 nm (Fig. S6B) shows a decrease at potentials below +0.20 V when the electrografting process is happening, either at AuSPE or CNDs/AuSPE. But, in the case of CNDs/AuSPE this decrease is greater, confirming that a higher amount of Azure A molecules is being electrografted when CNDs are present on the electrode surface. In both cases the voltabsorptograms derivatives vs. time (Fig. S6E) show a reversible peak at the same potential (E = +0.14 V) previously observed for the electroreduction of the aryl diazonium group (see CVs of Fig. 6C and D), what clearly shows the relationship between the spectroscopic changes and the electrochemical process. In the case of the absorbance at 630 nm, an increase in ΔAbs on successive CV scans can be observed. This band is related to the generation of non-diazotized Azure Aox on the electrode surface once the aryl diazonium electroreduction process occurs. At a first instance, when the electroreduction occurs the absorbance decreases, but then when the reduced form (Azure Ared) is oxidized back during the anodic scan the absorbance increases. This indicates that the initial Azure Aox diazotized form has been transformed into the non-diazotized Azure Aox form through the electrografting process and this specie adsorbs to the electrode surface. The ΔAbs increase is higher when no CNDs are present on the electrode surface (Fig. S6C, black line),

what could be due to the fact that the UV-Vis absorption band intensity is different when Azure A is grafted to gold or to carbon. The above results confirm the electrografting of Azure A on CNDs and provide new insights about the process.

The spectroelectrochemical response of Azure A modified electrodes (either electrografted or adsorbed on CNDs/AuSPE) was also studied in 0.1 M HCl (see Supporting Information, Fig. S7). The CV when Azure A is electrografted to the CNDs/AuSPEs shows a well-defined reversible process at E0 = 0.17 V. However, Azure A adsorbed on CNDs/AuSPE results in a poor defined redox pair at 0.05 V. The UV-Vis behavior in both cases shows that the absorbance at 590 nm and 630 nm decreases as the Azure Aox is reduced to Azure Ared, but the absorbance intensity variation is higher in the case of electrografted Azure A compared with adsorbed Azure A. This indicates that a higher amount of Azure A molecules are immobilized on the electrode surface using the electrografting protocol, corroborating what was observed in the CVs.

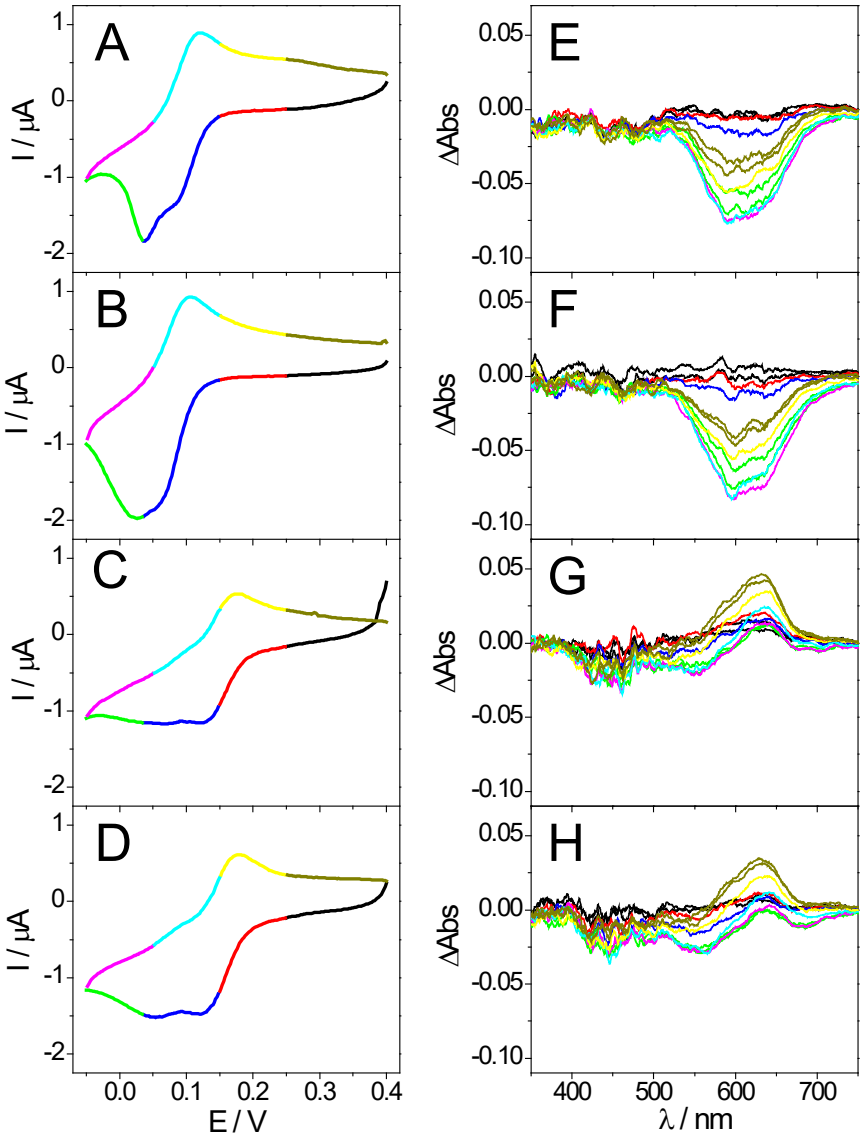

Figure 6. Cyclic voltammograms of 62.5 µM Azure A at AuSPE (A) or CNDs/AuSPE (B) and of 62.5 µM Azure A diazonium salt at AuSPE (C) or CNDs/AuSPE (D) in 0.1 M HCl at 0.01 Vs-1. Successive UV-Vis absorbance variation spectra associated with the cyclic voltammogram of

62.5 µM Azure A at AuSPE (E) or CNDs/AuSPE (F) and of 62.5 µM Azure A diazonium salt at AuSPE (G) or CNDs/AuSPE (H) in 0.1 M HCl.

One of the objectives of these investigations was the modification of CNDs with interesting compounds, such as dyes, to tune their intrinsic properties and explore new functions. We have previously reported on the electrocatalytic properties of Azure A modified electrodes toward the oxidation of the reduced form of β-nicotinamide adenine dinucleotide (NADH) [38]. In order to investigate the potential functions of the new Azure A modified nanomaterial prepared, taking advantage of the synergistic effects produced by combining the properties of a carbon nanomaterial and Azure A, its electrocatalytic activity towards the oxidation of hydrazine was assayed.

Fig. 7 shows cyclic voltammetry responses at 0.01 Vs-1 in pH 7.0 PB of electrodes modified with Azure A electrografted on CNDs (AA/CNDs/AuSPE) in absence and presence of 1.0 mM hydrazine. As can be observed after addition of 1.0 mM hydrazine, there is a dramatic increase in the anodic current. This behavior is consistent with a very strong electrocatalytic effect. As a comparison, oxidation of hydrazine under identical conditions at an unmodified gold electrode is also shown (curve c). The electrode modification with AA/CNDs results in a decrease of the overpotential of about 100 mV and an increase in current of about 26%.

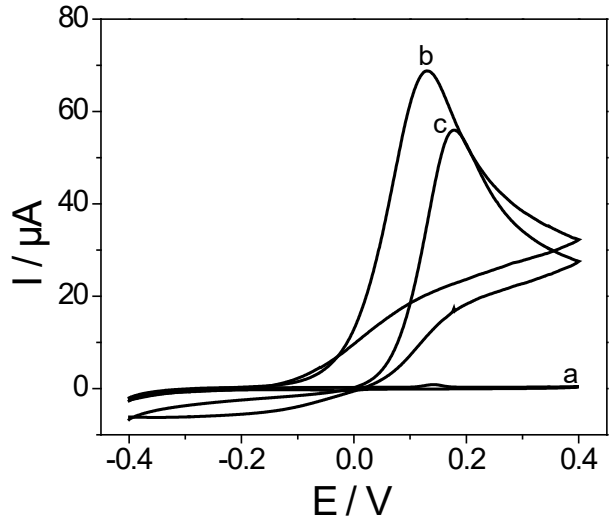

Figure 7. Cyclic voltammetric response of AA/CNDs modified grafted electrodes (b) and plain gold electrodes (c) in presence and absence (a) of 1.0 mM of hydrazine. Scan rate: 0.01 Vs-1.

4. Conclusions.

In summary, we have synthesized CNDs with enriched peripherical carboxylic groups from glucose. The obtained CNDs were assembled on AuSPE electrodes and functionalized with a phenothiazine by electrografting of Azure A diazonium salt. Characterization by cyclic voltammetry and spectroelectrochemistry confirms the covalent anchoring of Azure A to the immobilized CNDs. Spectroelectrochemical experiments allow us to obtain valuable data to achieve a better characterization of the electrografting process.

The potential application of the resulting chemically modified CNDs has been proved to the electrocatalytic oxidation of hydrazine. Based on our experiments, this is a highly reproducible synthesis method for the production of carboxylic carbon nanodots, which yields stable, fluorescent CNDs with functional groups that enable their chemical modification. In particular, through diazonium chemistry, which is a versatile, helpful and robust tool for the selective modification of CNDs with electroactive species interesting in many fields, such as sensors, biosensors, catalysis.

Acknowledgments

The authors acknowledge the Ministry of Economy and Competitiveness (project No. CTQ2014-53334-C2-1-R, CTQ2017-84309-C2-1-R and CTQ2015-71955-REDT) and Community of Madrid (NANOAVANSENS Program) for financial support.

References

[1] Xiangling, R.; Jing, L.; Xianwei, M.; Jianfei, W.; Tianlong, L.; Fangqiong, T. Synthesis of Ultra-Stable Fluorescent Carbon Dots from Polyvinylpyrrolidone and Their Application in the Detection of Hydroxyl Radicals. Chem. Asian. J. 2014, 9, 1054-1059.

[2] Li, H.;Kang, Z.;Liu, Y.; Lee, S.-T. Carbon nanodots: synthesis, properties and applications. J. Mater. Chem. 2012, 22, 24230-24253.

[3] Li, H.; He, X.; Liu, Y.; Huang, H.; Lian, S.; Lee, S.-T.; Kang, Z. One-step ultrasonic synthesis of water-soluble carbon nanoparticles with excellent photoluminescent properties. Carbon 2011, 49, 605-609.

[4] Baker, S. N.; Baker, G. A. Luminescent Carbon Nanodots: Emergent Nanolights. Angew. Chem.-Int. Edit. 2010, 49, 6726-6744.

[5] Esteves da Silva, J. C. G.; Gonçalves, H. M. R. Analytical and bioanalytical applications of carbon dots. Trac-Trends Anal. Chem. 2011, 30, 1327-1336.

[6] Xu, B.;Zhao, C.;Wei, W.;Ren, J.;Miyoshi, D.;Sugimoto, N.; Qu, X. Aptamer carbon nanodot sandwich used for fluorescent detection of protein. Analyst 2012, 137, 5483-5486.

[7] Zhu, S.; Meng, Q.;Wang, L.;Zhang, J.;Song, Y.;Jin, H.;Zhang, K.;Sun, H.;Wang, H.; Yang, B. Highly Photoluminescent Carbon Dots for Multicolor Patterning, Sensors, and Bioimaging. Angew. Chem.-Int. Edit. 2013, 52, 3953-3957.

[8] Xu, X.;Ray, R.;Gu, Y.;Ploehn, H. J.;Gearheart, L.;Raker, K.; Scrivens, W. A. Electrophoretic Analysis and Purification of Fluorescent Single-Walled Carbon Nanotube Fragments. J. Am. Chem. Soc. 2004, 126, 12736-12737.

[9] Lim, S. Y.;Shen, W.; Gao, Z. Carbon quantum dots and their applications. Chem. Soc. Rev. 2015, 44, 362-381.

[10] Zhao, A.;Chen, Z.;Zhao, C.;Gao, N.;Ren, J.; Qu, X. Recent advances in bioapplications of C-dots. Carbon 2015, 85, 309-327.

[11] Arcudi, F.; Đorđević, L.; Prato, M. Synthesis, Separation, and Characterization of Small and Highly Fluorescent Nitrogen-Doped Carbon NanoDots. Angew. Chem.-Int. Edit. 2016, 55, 2107-2112.

[12] Arcudi, F.; Đorđević, L.; Prato, M. Synthesis, Separation, and Characterization of Small and Highly Fluorescent Nitrogen-Doped Carbon NanoDots. Angew. Chem.-Int. Edit. 2016, 128, 2147-2152.

[13] Ferrer-Ruiz, A.; Scharl, T.;Haines, P.;Rodríguez-Pérez, L.;Cadranel, A.;Herranz, M. Á.;Guldi, D. M.; Martín, N. Exploring Tetrathiafulvalene–Carbon Nanodot Conjugates in Charge Transfer Reactions. Angew. Chem.-Int. Edit.2018, 57, 1001-1005.

[14] Pinson, J.; Podvorica, F. Attachment of organic layers to conductive or semiconductive surfaces by reduction of diazonium salts. Chem. Soc. Rev. 2005, 34, 429-439.

[15] Allongue, P.; Delamar, M.; Desbat, B.;Fagebaume, O.; Hitmi, R.;Pinson, J.; Savéant, J.-M. Covalent Modification of Carbon Surfaces by Aryl Radicals Generated from the Electrochemical Reduction of Diazonium Salts. J. Am. Chem. Soc. 1997, 119, 201-207.

[16] Brooksby, P. A.; Downard, A. J. Electrochemical and Atomic Force Microscopy Study of Carbon Surface Modification via Diazonium Reduction in Aqueous and Acetonitrile Solutions. Langmuir 2004, 20, 5038-5045.

[17] Delamar, M.; Désarmot, G.; Fagebaume, O.; Hitmi, R.; Pinsonc, J.; Savéant, J. M. Modification of carbon fiber surfaces by electrochemical reduction of aryl diazonium salts: Application to carbon epoxy composites. Carbon 1997, 35, 801-807.

[18] Downard Alison, J. Electrochemically Assisted Covalent Modification of Carbon Electrodes. Electroanalysis 2000, 12, 1085-1096.

[19] Downard, A. J.; Prince, M. J. Barrier Properties of Organic Monolayers on Glassy Carbon Electrodes. Langmuir 2001, 17, 5581-5586.

[20] Kariuki, J. K.; McDermott, M. T. Nucleation and Growth of Functionalized Aryl Films on Graphite Electrodes. Langmuir 1999, 15, 6534-6540.

[21] Ortiz, B.; Saby, C.;Champagne, G. Y.; Bélanger, D. Electrochemical modification of a carbon electrode using aromatic diazonium salts. 2. Electrochemistry of 4-nitrophenyl modified glassy carbon electrodes in aqueous media. J. Electroanal. Chem.1998, 455, 75-81.

[22] Ranganathan, S.; Steidel, I.; Anariba, F.; McCreery, R. L. Covalently Bonded Organic Monolayers on a Carbon Substrate: A New Paradigm for Molecular Electronics. Nano Lett. 2001, 1, 491-494.

[23] Saby, C.;Ortiz, B.;Champagne, G. Y.; Bélanger, D. Electrochemical Modification of Glassy Carbon Electrode Using Aromatic Diazonium Salts. 1. Blocking Effect of 4-Nitrophenyl and 4-Carboxyphenyl Groups. Langmuir 1997, 13, 6805-6813.

[24] Belanger, D.; Pinson, J. Electrografting: a powerful method for surface modification. Chem. Soc. Rev. 2011, 40, 3995-4048.

[25] Xu, Y.;Liu, J.;Zhang, J.;Zong, X.;Jia, X.;Li, D.; Wang, E. Chip-based generation of carbon nanodots via electrochemical oxidation of screen printed carbon electrodes and the

applications for efficient cell imaging and electrochemiluminescence enhancement. Nanoscale 2015, 7, 9421-9426.

[26] Martínez-Periñán, E.;Bravo, I.;Rowley-Neale Samuel, J.;Lorenzo, E.; Banks Craig, E. Carbon Nanodots as Electrocatalysts towards the Oxygen Reduction Reaction. Electroanalysis 2018, 30, 436-444.

[27] Shao, X.; Gu, H.;Wang, Z.;Chai, X.;Tian, Y.; Shi, G. Highly Selective Electrochemical Strategy for Monitoring of Cerebral Cu2+ Based on a Carbon Dot-TPEA Hybridized Surface. Anal. Chem. 2013, 85, 418-425.

[28] Roushani, M.; Sarabaegi, M. Novel electrochemical sensor based on carbon nanodots/chitosan nanocomposite for the detection of tryptophan. J. Iran Chem. Soc. 2015, 12, 1875-1882.

[29] García-Mendiola, T.;Bravo, I.;López-Moreno, J. M.;Pariente, F.;Wannemacher, R.;Weber, K.;Popp, J.; Lorenzo, E. Carbon nanodots based biosensors for gene mutation detection. Sens. Actuator B-Chem .2018, 256, 226-233.

[30] Garoz-Ruiz, J.;Heras, A.;Palmero, S.; Colina, A. Development of a Novel Bidimensional Spectroelectrochemistry Cell Using Transfer Single-Walled Carbon Nanotubes Films as Optically Transparent Electrodes. Anal. Chem. 2015, 87, 6233-6239.

[31] Hansen, W. N.; Osteryoung, R. A.; Kuwana, T. Internal Reflection Spectroscopic Observation of Electrode-Solution Interface. J. Am. Chem. Soc.1966, 88, 1062-1063.

[32] Heineman, W. R. Spectroelectrochemistry. Combination of optical and electrochemical techniques for studies of redox chemistry. Anal. Chem.1978, 50, 390A-402A.

[33] Peng, H.; Travas-Sejdic, J. Simple Aqueous Solution Route to Luminescent Carbogenic Dots from Carbohydrates. Chem. Mat. 2009, 21, 5563-5565.

[34] Horcas, I.; Fernández, R.;Gómez-Rodríguez, J. M.; Colchero, J.; Gómez-Herrero, J.; Baro, A. M. WSXM: A software for scanning probe microscopy and a tool for nanotechnology. Rev. Sci. Instrum. 2007, 78, 013705.

[35] Zhu, S.; Song, Y.; Zhao, X.; Shao, J.;Zhang, J.; Yang, B. The photoluminescence mechanism in carbon dots (graphene quantum dots, carbon nanodots, and polymer dots): current state and future perspective. Nano Res. 2015, 8, 355-381.

[36] Bernard, M.-C.; Chaussé, A.; Cabet-Deliry, E.; Chehimi, M. M.;Pinson, J.;Podvorica, F.; Vautrin-Ul, C. Organic Layers Bonded to Industrial, Coinage, and Noble Metals through Electrochemical Reduction of Aryldiazonium Salts. Chem. Mat. 2003, 15, 3450-3462.

[37] Mažeikienė, R.; Niaura, G.; Eicher-Lorka, O.; Malinauskas, A. Raman spectroelectrochemical study of Toluidine Blue, adsorbed and electropolymerized at a gold electrode. Vib. Spectrosc. 2008, 47, 105-112.

[38] Revenga-Parra, M.; Gómez-Anquela, C.;García-Mendiola, T.;Gonzalez, E.;Pariente, F.; Lorenzo, E. Grafted Azure A modified electrodes as disposable β-nicotinamide adenine dinucleotide sensors. Anal. Chim. Acta. 2012, 747, 84-91.

[39] Bishop, E. CHAPTER 8B - Oxidation-Reduction indicators of high formal potential. In Indicators. Pergamon, 1972; pp 531-684.

[40] Laviron, E. General expression of the linear potential sweep voltammogram in the case of diffusionless electrochemical systems. J. Electroanal. Chem. Interfacial Electrochem. 1979, 101, 19-28.